"Physics of Auroral Phenomena", Proc. XXXI Annual Seminar, Apatity, pp. 61- 64, 2008

Polar Geophysical Institute

USING MODELS OF MAGNETOSPHERIC MAGNETIC FIELD FOR REAL-TIME ASSESSMENT OF GEOMAGNETIC ACTIVITY BASED ON CHAMP MAGNETIC MEASUREMENT

L.I. Gromova, L.A. Dremukhina, A.E. Levitin, E.G. Avdeeva *(Pushkov Institute of Terrestrial Magnetism, Ionosphere and Radio Wave Propagation, Troitsk, Moscow Region, Russia)*

Abstract. The method of real-time assessment of geomagnetic activity based on satellite magnetic measurements is presented. Satellite data of the magnetic field module and/or its components measured along each orbit (or any of its segments) are compared with magnetic field model. Output of the model depends on geomagnetic activity states (quiet, weakly disturbed, disturbed, strongly disturbed conditions) which may be defined by different way. To determine geomagnetic activity for some time interval, satellite data of the magnetic field module and/or its components measured along orbit (or any of its segments) covered this interval should be compared with magnetic field model outputs for different states of geomagnetic activity. The best agreement between observed data and model output determines geomagnetic activity state of the time interval. We used the magnetic field measurements of CHAMP satellite and modern models of the magnetospheric magnetic field such as Paraboloid model and Tsyganenko's model T96 for monitoring of the geomagnetic activity state for some time interval covered by CHAMP data.

Introduction

The negative effect of Space weather on cosmic and ground-based technical systems can be weakened by using the real-time assessment of geomagnetic activity. The magnetic field measurements by low-orbiting satellites and modern magnetospheric magnetic field models may be used for real-time monitoring of the geomagnetic field and, as a result, the geomagnetic activity state for some time interval. The intensity of the geomagnetic field may be described by different indices, among them planetary indices *Kp* and *Ap* are the most common. Table 1 presents example of geomagnetic activity classification according to geomagnetic indices *Kp* and *Ap* [*http://www.astrosurf.com/luxorion*].

Table 1. Classification of geomagnetic activity according to Kp and Ap indices of geomagnetic activity

Classification of geomagnetic activity		
Ap Index	*Kp* index	Activity
0 - 7	0 - 1	Quiet
8 - 15	2 - 3	Unsettled
16 - 29	4	Active
30 - 49	5	Minor Storm
50 - 99	6	Major Storm
100 - 400	7 - 9	Severe Storm

For our study we have fixed four states of geomagnetic activity:

*Q*uiet (Q) for $0 \le Kp < 3$,
*W*eakly *D*isturbed (WD) for $3 \le Kp < 5$,
*D*isturbed (D) for $5 \le Kp < 7$,
*S*trong *D*isturbed (SD) for $Kp \ge 7$.

We have used two modern models of the magnetospheric magnetic field such as Paraboloid model (PM) created in Skobeltsyn Institute of Nuclear Physics of MSU [*Feldstein et al.,* 2005] and Tsyganenko's model T96[*Tsyganenko,* 1996, and *http://geo.phys.spbu.ru/~tsyganenko/T96.html*]**.** They allow to describe the distribution of the geomagnetic field components in any given point of the near-Earth's space depending on model input parameters. As the magnetospheric magnetic field models are parameterized by Solar Wind/Interplanetary Magnetic Field and/or indices of geomagnetic activity, these external parameters have been arranged into groups according to chosen geomagnetic activity states. Satellite data of the magnetic field module and/or its components measured along each orbit (or any of its segments) are compared with model outputs calculated for each states of geomagnetic activity indicated above.
Some results of using the magnetic field measurements of CHAMP satellite and the magnetospheric magnetic field models PM and T96 for real-time monitoring of the geomagnetic activity states are presented.

CHAMP measurements and model input parameters

To use CHAMP measurements for real-time describing the geomagnetic activity state for some time interval, the Main magnetic field of the Earth has been modeled by IGRF2005 coerced to measurement date taking into account the model of the secular variation. These values have been subtracted from Champ vector measurements of the magnetic field. To create a model of the magnetic field CHAMP data have been smoothed by running average with step equal 81 [*Filippov et al.,* 2006]. The magnetic field data measured by CHAMP are available from May 1, 2001 until December 31, 2005.
The magnetospheric magnetic field modeled by PM and T96 are parameterized by *By* and *Bz* IMF-components, velocity(*V*), density (*N*), and dynamic pressure (*P*) of Solar wind (*SW*), *Dst* and *AL* indices of geomagnetic activity. To determine model input parameters we have used data available from OMNI Web system (http://omniweb.gsfc.nasa. gov) and World Data Center for Geomagnetism, Kyoto (http://swdwww.Kugi.Kyoto-

u.ac.jp) during 1997-2006. From IMF, SW and geomagnetic indices data we included in our study 81944 hours when *Bz, By, V, N, P, Dst, AL* data was available simultaneously. *Kp* values were in the form 0, 0+,1+, 2-, 2, 2+..., OMNIWeb system presents 3-hourly Kp values assigned to each hour of the relevant 3-hour interval. Hourly data of *Bz, By, V, N, P, Dst, AL* data were arranged into 9 groups according to *Kp* changing per 1 and averaged within each group (see Table 2).

Table 2. Parameters of interplanetary magnetic field and solar wind, geomagnetic activity indices for the time interval from 1997 to 2006 averaged within each group according to Kp changing per 1.

Kp	Number of available data	By	Bz	N	V	P	Dst	AL
0 ÷ 1-	14848	-0.007	1.320	5.694	376	1.386	-6	-25
1 ÷ 2-	21989	0.023	0.606	5.859	411	1.688	-10	-55
2 ÷ 3-	20180	0.028	-0.40	5.966	454	2.048	-16	-110
3 ÷ 4-	14434	0.152	-0.728	6.338	501	2.529	-24	-188
4 ÷ 5-	6870	0.522	-1.545	6.921	539	3.186	-35	-298
5 ÷ 6-	2402	1.092	-2.960	8.163	555	4.064	-50	-397
6 ÷ 7-	868	1.400	-4.610	9.165	567	5.487	-75	-517
7 ÷ 8-	360	2.749	-5.709	10.828	631	7.988	-113	-583
> 8	144	1.882	-14.177	12.946	727	13.559	-167	-782

Table 3 presents IMF and SW parameters and indices of geomagnetic activity used as inputs of the magnetospheric magnetic field models averaged for each group according to the states of geomagnetic activity fixed above.

Table 3. Parameters of interplanetary magnetic field and solar wind, geomagnetic activity indices averaged for each group according to fixed states of geomagnetic activity.

Kp	Geomagnetic activity state and number of available data		By	Bz	N	V	P	Dst	AL
0 ÷ 3-	Quiet (Q)	56866	0.017	0.563	5.854	417	1.737	-11	-66
3 ÷ 5-	Weakly disturbed (WD)	21304	0.271	-0.992	6.451	514	2.741	-28	-223
5 ÷ 7-	Disturbed (D)	3270	1.174	-3.389	8.429	559	4.442	-57	-429
> 7	Strong disturbed (SD)	504	2.502	-8.429	11.433	658	9.580	-129	-640

Real-time monitoring of the geomagnetic activity levels

For real-time monitoring of the geomagnetic activity level we processed data of 22 3-hourly time intervals during November 2004-February 2005 covered by CHAMP data. As orbital period of CHAMP is approximately 94 min**,** two CHAMP passes cover 3-hourly interval. Abrupt change of high-latitude magnetic field may occur under different level of geomagnetic activity and any model is not able to describe real field measured by satellites rather plausibly, therefore only middle-latitudinal segments of CHAMP passes have been chosen for modeling.

Model magnetic field was calculated for each point of middle-latitudinal segments of CHAMP passes covered chosen time interval and for quiet, weakly disturbed, disturbed, strong disturbed states described at Table 2. Model outputs were averaged. For each time interval state of geomagnetic activity is determined as state for which the discrepancy between averaged module of measured magnetic field and averaged module of the magnetic field modeled is minimum.

Tables 4 and 5 present results of real-time describing geomagnetic activity whenestimated state of geomagnetic activity coincides with the state corresponding to *Kp*-index for the same time interval. It is shown discrepancies between model's outputs and CHAMP magnetic field data for quiet, weakly disturbed, disturbed and strong disturbed states. Minimum discrepancies, selected by BOLD, determine estimated states of geomagnetic activity.

Table 4. Real-time assessment of geomagnetic activity based on PM model of the magnetospheric magnetic field.

Date	UT	*Kp* *(State)*	Discrepancy between model and observed magnetic field			
			Quiet (*Q*)	Weakly disturbed (WD)	Disturbed (*D*)	Strong Disturbed (*SD*)
10.11.04	00-02	8- (*SD*)	164.97	161.99	151.70	**124.23**
05.01.08	00-02	7 (*SD*)	97.67	93.65	81.20	**56.53**
10.01.05	00-02	1- (*Q*)	**18.74**	20.11	23.49	54.83
18.01.05	00-02	7 (*SD*)	72.47	68.97	58.34	**37.44**
14.02.05	00-02	1- (*Q*)	**15.08**	15.78	22.28	55.26
16.02.05	00-02	3 (*WD*)	13.42	**12.97**	15.81	45.52
24.02.05	00-02	0 (*Q*)	**7.79**	10.71	23.25	61.48

Table 5. Real-time assessment of geomagnetic activity based on T96 model of the magnetospheric magnetic field

Date	UT	*Kp*	Discrepancy between model and observed magnetic field			
			Quiet(*Q*)	Weakly disturbed (WD)	Disturbed (*D*)	Strong disturbed (*SD*)
10.11.04	00-02	8- (*SD*)	147.09	123.65	84.66	**40.22**
25.11.04	00-02	4 (*WD*)	38.00	**20.50**	31.48	124.59
04.12.04	00-02	0 (*Q*)	**5.86**	18.52	57.44	153.52
12.12.04	00-02	5- (*WD*)	26.06	**18.18**	41.92	134.42
18.12.04	00-02	4+ (*WD*)	16.05	**12.49**	46.29	140.02
26.12.04	00-02	3- (*Q*)	**11.11**	17.73	52.29	148.47
02.01.05	00-02	4+ (*WD*)	42.64	**20.23**	25.80	116.09
10.01.05	00-02	1- (*Q*)	**9.22**	19.04	55.65	148.18
14.01.05	00-02	3- (*Q*)	**13.25**	15.01	50.25	143.18
21.01.05	00-02	3+ (*WD*)	21.07	**10.21**	40.56	134.40
26.01.05	00-02	1- (*Q*)	**9.28**	15.09	51.62	145.18
05.02.05	00-02	0+ (*Q*)	**5.29**	26.87	66.19	163.07
14.02.05	00-02	1- (*Q*)	**4.79**	26.30	64.10	156.58
24.02.05	00-02	0 (*Q*)	**17.29**	40.82	80.00	176.11

As it is shown in Table 3 and Table 4 using PM model allows to predict state of geomagnetic activity for 32% events of study and T96 model gives correct assessment of geomagnetic activity state for 64% ones.

Figure 1 shows the module of the magnetic field measured by CHAMP and the module of magnetic field calculated using PM and T96 models for events under strong disturbed state and quiet states of geomagnetic activity Events have been chosen according to Table 3 and Table 4. States of geomagnetic activity of the interval are predicted correctly by the both models.

Discussion and conclusions

Real-time monitoring of the geomagnetic field states allows to describe electromagnetic situation in the near-Earth's space. It may be used for ground-based and cosmic geophysical experiments and for solving applied problem such as weakening of the negative effect of Space weather on cosmic and ground-based technical systems. Except for real-time monitoring of the geomagnetic activity state, suggested method may be used for describing the thermospheric density variation that may considerably change parameters of satellite orbit.

Reaction of the thermosphere to changing geomagnetic conditions occurs through a series of complex and interdependent processes. In response to energy and momentum deposition at high latitudes in the form of Joule heating, particle precipitation, and electric fields that drive neutral winds via ion-neutral collisions, a global circulation system is set up to redistribute mass, momentum, and energy. Depending on molecular weight, the various constituents (O, O_2, N_2, H, He) respond differently to wind and temperature perturbations. The ionospheric plasma and neutral thermosphere respond interactively and nonlinearly with each other, through chemical, dynamical, and electrodynamical pathways. Nitric oxide (*NO*) production is greatly enhanced at high latitudes, and the NO, which is an efficient radiative cooler, is transported equatorward by the fortified wind system. In addition, waves ranging in scale from hundreds to thousands kilometers propagate toward low latitudes and also act to redistribute heat and momentum. Ultimately, much of the excess energy deposited into the thermosphere during a magnetic storm is radiated to space in the infrared (mostly by *NO* and CO_2). The relationship between geomagnetic disturbances and thermospheric composition, density, and winds has been studied in depth for decades. The first discoveries of this connection resulted from discrepancies between predicted and observed satellite ephemerides during periods of geomagnetic activity. Models for predicting thermospheric density derived from satellite drag data. One of the instruments on CHAMP is a sensitive triaxial accelerometer that is capable of providing estimates of total mass density and cross-track winds. With a near-polar inclination, the satellite provides near-global coverage at an approximate altitude of 410 km within two local time sectors at most latitudes. On board the CHAMP satellite is the accelerometer, which measures the sum of all forces on the satellite's surface. This measured quantity is comprised mostly of the force imparted to the satellite by atmospheric drag, with lesser constituents such as solar and Earth radiation pressure also contributing. According to CHAMP measurements during times of extreme geomagnetic activity, thermosphere densities near 410km exhibit enhancements of 200–300%[*Bruinsma et al.*, 2006].

The data of thermospheric density measured by CHAMP satellite during long time allow to relate the termospheric density variation with above indicated geomagnetic activity states caused possible changing parameters of a satellite orbit. The suggested method of real-time assessment of geomagnetic activity may be developed to create a real-time assessment of changing parameters of a satellite orbit with perigee altitudes closed to thermosphere altitudes.

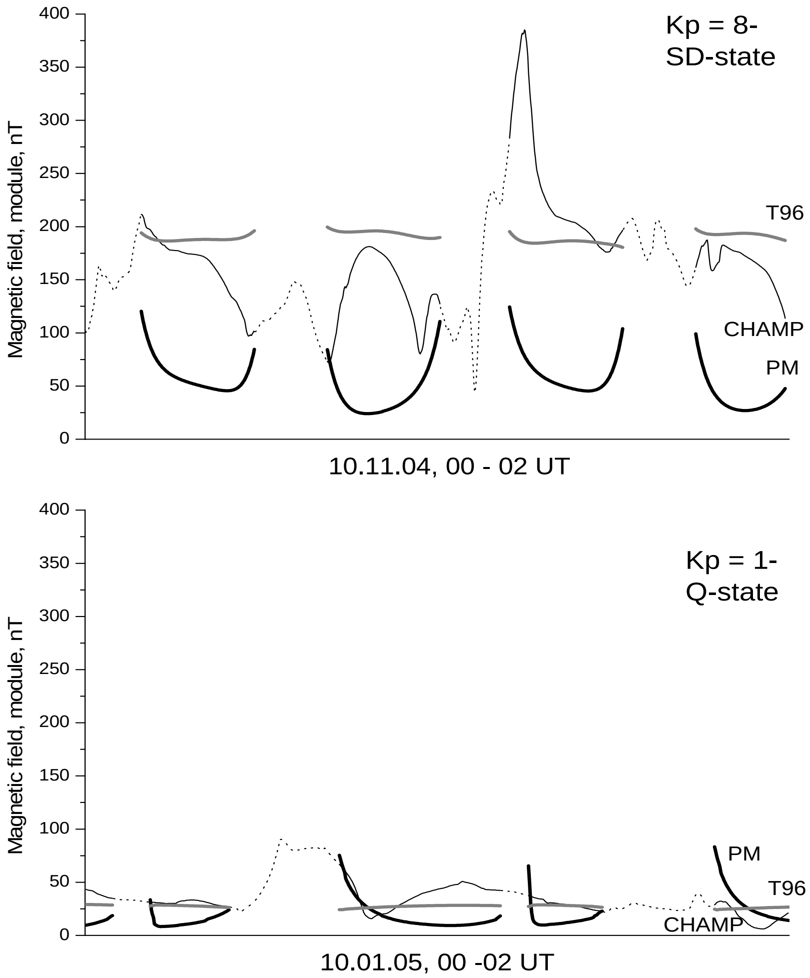

Figure 1. Module of the magnetic field measured by Champ (thin solid line + thin dotted line), module of PM magnetic field (thick black line) and module of the T96 magnetic field (thick grey line) for time interval of different geomagnetic activity states (from top to bottom): strong disturbed state (SD) and quiet state (Q). States of geomagnetic activity of the interval is predicted correctly by the both models. Thin solid lines mark middle-latitude segments of CHAMP passes chosen for modeling and comparison.

Acknowledgments. This study is supported by RFBR grants 07-05-13524, 08-05-00896,

References

1. Bruinsma, S., J. Forbes, R. Nerem, X. Zhang, Thermospheric density response to the 20-21 November 2003 solar and geomagnetic storm from CHAMP and GRACE accelerometer data, J. Geophys. Res., 111, A06303, doi:10.1029/2005JA011284,2006

2. Feldstein, Y. I.; Levitin, A. E.; Kozyra, J. U.; Tsurutani, B. T.; Prigancova, A.; Alperovich, L.; Gonzalez, W. D.; Mall, U.; Alexeev, I. I.; Gromova, L. I.; Dremukhina, L. A., Self-consistent modeling of the large-scale distortions in the geomagnetic field during the 24–27 September 1998 major magnetic storm., *J. Geophys. Res.,* 110, A11, A11214 10.1029/2004JA010584, 2005.

3. Filippov S. V., A. E. Levitin, L. I. Gromova, T. I. Zvereva, M. A. Ivanova, Geomagnetic field real state describing by satallite magnetic measurenemts, *Proc. of First International science meeting SWARM*, 3-5 May, 2006, Nantes, France, 2006.

4. Levitin A.E., Dremukhina L.A., Gromova L.I., Avdeeva E.G., Korzhan D.I., Real-time assessment of geomagnetic activity based on satellite magnetic field measurements, *Physics of auroral phenomena, February-March 2007*, Apatity, 2007

5. Tsyganenko, N. A., Effect of solar wind conditions on the global magnetosheric configuration as deduced from data-based field models, Rus. Space Agensy Spec. Publ., ESA SP-389, 181, 1996.